International Publication House Open (IPHO)
https://www.iphopen.org/ms

On the Odd Burr III-Type II Generalized Exponential-G Family of Distributions: Properties with Applications to Failure Data

September 12, 2025

Abstract

This study introduces the odd Burr III-Type II Generalized Exponential-G (OBIII-TIIGE-G) family of distributions, a flexible statistical framework designed to model diverse data geometries. By synthesizing the structural strengths of the odd Burr III-G and the type II general exponential-G families, the proposed model addresses critical gaps in existing distributions, particularly their inability to simultaneously capture monotonic and non-monotonic hazard rates. The OBIII-TIIGE-G family offers analytical tractability, with closed-form expressions for quantile functions, moments, and hazard rate dynamics, enabling robust reliability assessments. Monte Carlo simulations validate the consistency and efficiency of maximum likelihood estimators, showing reduced bias and root mean square error as sample sizes increase. Applied to real-world failure datasets—carbon fiber breaking stress and silicon nitride fracture toughness, the model demonstrates superior goodness-of-fit over six competing distributions, evidenced by lower goodness-of-fit statistics with higher p-values. Its ability to adapt to symmetric, skewed, and heavy-tailed data, coupled with identifiable parameters and precise estimation, positions it as a vital tool for reliability engineering and materials science. This research advances distribution theory and provides practitioners with a versatile solution for modeling complex failure-time phenomena.

Keywords: Odd Burr III-G; Type II General Exponential-G; Hazard rate; Moments; Maximum likelihood estimation; Simulations; Goodness-of-fit.
Mathematics Subject Classification 62E99, 60E05

DOI:- 10.5281/zenodo.15743517 | Manuscript ID # 302

1 Introduction

Recent advancements in statistical distribution theory have emphasized the development of flexible families of distributions to model complex real-world phenomena, in diverse domains including reliability engineering, meteorology, and survival analysis.

The odd Burr III-G (OBIII-G) family, proposed by Alizadeh et al. [3], extends the Burr type III distribution, providing greater flexibility to model complex data patterns, heavy-tailed phenomena, and diverse hazard rate trends. This generalization enhances its applicability across various domains. This remarkable flexibility and adaptability are precisely why the OBIII-G generator has been extensively generalized and modified in recent literature. Some of its extensions include Marshall-Olkin odd Burr III-G by Afify et al. [1], odd Burr III negative binomial family by Jamal et al. [9], type I heavy-tailed Burr III family by Nkomo et al. [14] and the exponentiated half-logistic odd Burr III-G family by Oluyede et al. [15], to mention just a few.

The type II general exponential-G (TIIGE-G) family, proposed by Hamedani et al. [7], have gained prominence for their ability to generalize baseline distributions through shape and scale parameters, enhancing their adaptability to diverse data behaviors. These families are celebrated for their mathematical tractability and capacity to model asymmetrical datasets. However, despite their versatility, existing distributions often face limitations in accommodating datasets with mixed skewness, symmetry, or extreme-value characteristics.

A notable research opportunity lies in merging different families of distributions, which can help address the challenges of modeling complex datasets and improve the accuracy and flexibility of analytical models. While the OBIII-G family excels in handling asymmetry and heavy-tailed behaviours, and the TIIGE-G family offers a robust framework for exponential-tail behavior, their standalone formulations may lack the structural synergy required to address datasets exhibiting complex behaviours necessitating a more versatile hybrid approach. Furthermore, many existing distributions fail to provide closed-form expressions for key statistical properties like quantile functions and moments, limiting their applicability in real-time reliability assessments and stochastic modeling.

To bridge these gaps, this study introduces the odd Burr III-type II generalized exponential-G (OBIII-TIIGE-G) family, a unified framework that synthesizes the strengths of the OBIII-G and TIIGE-G families. By replacing the baseline distribution in the OBIII-G structure with the TIIGE-G model, the proposed family achieves enhanced flexibility in hazard rate modeling, accommodates diverse density geometries including J-shaped, symmetric, and asymmetric patterns, and retains analytical tractability for moments, quantiles, and parameter estimation. Through extensive simulations and applications to

failure-time datasets, the OBIII-TIIGE-G family demonstrates superior performance over competing models, addressing a critical need for adaptable tools in reliability analysis, risk assessment, and survival studies. This innovation not only extends the theoretical boundaries of distribution theory but, also provides practitioners with a robust statistical toolkit for complex data scenarios.

The paper is organized as follows: Section 2 introduces the generalized family of distributions (FoD), presenting its cumulative and density functions. Section 3 derives key statistical properties (quantile function, density expansions, moments), while Section 4 explores special cases of the family. Section 5 addresses parameter estimation via maximum likelihood and validates the framework's robustness through Monte Carlo simulations. Section 6 showcases the model's empirical superiority using failure-time datasets, outperforming competing distributions. The study culminates in Section 7 with synthesis, conclusions, and forward-looking research directions.

2 The new family of distributions

Alizadeh et al. [3] developed the odd Burr III-G (OBIII-G) FoD, which has a cumulative distribution function (cdf)

$$\begin{aligned} F(x;\beta,k,\phi) &= \int_0^{\frac{G(x;\phi)}{(1-G(x;\phi))}} \beta k t^{-\beta-1}(1+t^{-\beta})^{-k-1}dt \\ &= \left[1+\left(\frac{1-G(x;\phi)}{G(x;\phi)}\right)^{\beta}\right]^{-k}, \end{aligned} \tag{1}$$

and probability density function (pdf)

$$f(x;\beta,k,\phi) = \beta k g(x;\phi)\frac{[1-G(x;\phi)]^{\beta-1}}{G(x;\phi)^{\beta+1}}\left[1+\left(\frac{1-G(x;\phi)}{G(x;\phi)}\right)^{\beta}\right]^{-k-1} \tag{2}$$

respectively, where $\beta, k > 0$ are shape parameters, $x > 0$ and ϕ is a parameter vector from the baseline distribution $G(.)$.

Hamedani et al. [7] proposed the type II general exponential (TIIGE-G) FoD with the cdf and pdf given by

$$F(x;\alpha,\lambda,\phi) = 1-\exp\left(\lambda\left[1-\left(\bar{G}(x;\phi)\right)^{-\alpha}\right]\right) \tag{3}$$

and

$$f(x;\alpha,\lambda,\phi) = \lambda\alpha g(x;\phi)\bar{G}^{-(\alpha+1)}(x;\phi)\exp\left(\lambda\left[1-\left(\bar{G}(x;\phi)\right)^{-\alpha}\right]\right), \tag{4}$$

respectively, where $\alpha > 0$ and $\lambda > 0$ are shape and scale parameters respectively, $x > 0$ and parameter vector ϕ from the baseline distribution $G(.)$, where $\bar{G}(x;\phi) = 1 - G(x;\phi)$.

Replacing the baseline cdf in Equation (1) with the TIIGE-G distribution yields a new FoD called the odd Burr III-type II general exponential-G (OBIII-TIIGE-G) distribution with cdf, survival function and pdf given by

$$F(x;\alpha,\lambda,\beta,k,\phi) = \left[1 + \left(\frac{\exp\left(\lambda\left[1-\left(\bar{G}(x;\phi)\right)^{-\alpha}\right]\right)}{1-\exp\left(\lambda\left[1-\left(\bar{G}(x;\phi)\right)^{-\alpha}\right]\right)}\right)^{\beta}\right]^{-k}, \quad (5)$$

$$S(x;\alpha,\lambda,\beta,k,\phi) = 1 - \left[1 + \left(\frac{\exp\left(\lambda\left[1-\left(\bar{G}(x;\phi)\right)^{-\alpha}\right]\right)}{1-\exp\left(\lambda\left[1-\left(\bar{G}(x;\phi)\right)^{-\alpha}\right]\right)}\right)^{\beta}\right]^{-k}, \quad (6)$$

and

$$\begin{aligned} f(x;\alpha,\lambda,\beta,k,\phi) &= \beta k\lambda\alpha g(x;\phi)\left(\bar{G}(x;\phi)\right)^{-(\alpha+1)} \frac{\left[\exp\left(\lambda\left[1-\left(\bar{G}(x;\phi)\right)^{-\alpha}\right]\right)\right]^{\beta}}{\left[1-\exp\left(\lambda\left[1-\left(\bar{G}(x;\phi)\right)^{-\alpha}\right]\right)\right]^{\beta-1}} \\ &\times \left[1 + \left(\frac{\exp\left(\lambda\left[1-\left(\bar{G}(x;\phi)\right)^{-\alpha}\right]\right)}{1-\exp\left(\lambda\left[1-\left(\bar{G}(x;\phi)\right)^{-\alpha}\right]\right)}\right)^{\beta}\right]^{-k-1} \end{aligned} \quad (7)$$

respectively, for $\alpha,\lambda,\beta,k,x > 0$ and parameter vector ϕ from the baseline distribution. The hrf of the OBIII-TIIGE-G FoD is then given by

$$\begin{aligned} h(x;\alpha,\lambda,\beta,k,\phi) &= \beta k\lambda\alpha g(x;\phi)\left(\bar{G}(x;\phi)\right)^{-(\alpha+1)} \frac{\left[\exp\left(\lambda\left[1-\left(\bar{G}(x;\phi)\right)^{-\alpha}\right]\right)\right]^{\beta}}{\left[1-\exp\left(\lambda\left[1-\left(\bar{G}(x;\phi)\right)^{-\alpha}\right]\right)\right]^{\beta-1}} \\ &\times \left[1 + \left(\frac{\exp\left(\lambda\left[1-\left(\bar{G}(x;\phi)\right)^{-\alpha}\right]\right)}{1-\exp\left(\lambda\left[1-\left(\bar{G}(x;\phi)\right)^{-\alpha}\right]\right)}\right)^{\beta}\right]^{-1} \end{aligned} \quad (8)$$

for $\alpha,\lambda,\beta,k,x > 0$ and parameter vector ϕ. It is essential to recognize that sub-families of the OBIII-TIIGE-G FoD can be delineated by systematically fixing individual parameters and their corresponding combinations to unit values.

3 Statistical properties

In this section, we will derive some statistical properties of the OBIII-TIIGE-G FoD. These properties will encompass the quantile function, density expansion, moments, and incomplete moments.

3.1 Quantile Function

To derive the quantile function of OBIII-TIIGE-G FoD, $Q_X(u)$, we invert the cdf given in Equation (5). Thus,

$$u = \left[1 + \left(\frac{\exp\left(\lambda\left[1-\left(\bar{G}(x;\phi)\right)^{-\alpha}\right]\right)}{1-\exp\left(\lambda\left[1-\left(\bar{G}(x;\phi)\right)^{-\alpha}\right]\right)}\right)^{\beta}\right]^{-k}, \tag{9}$$

where where $p \sim U(0,1)$. Consequently, the quantile function of OBIII-TIIGE-G FoD is

$$Q_X(u) = G^{-1}\left(1 - \left[1 - \left(\frac{\lambda\left(u^{-\frac{1}{k}}-1\right)^{\frac{1}{\beta}}}{1+\left(u^{-\frac{1}{k}}-1\right)^{\frac{1}{\beta}}}\right)\right]^{\frac{1}{\alpha}}\right) \tag{10}$$

The quantile function exists when the parent distribution $G(.)$ is specified. This allows generating random variates by setting $p \sim U(0,1)$. The quantile function permits direct calculation of key distributional characteristics, that is, the lower quartile ($Q_{0.25}$ or 25^{th} percentile), the median ($Q_{0.5}$ or 50^{th} percentile) and the upper quartile ($Q_{0.75}$, or 75^{th} percentile).

3.2 Density expansion

Considering the generalized binomial series expansions, $(1-x)^k = \sum_{i=0}^{\infty}(-1)^i\binom{k}{i}x^i$, $(1-x)^{-k} = \sum_{i=0}^{\infty}\binom{k+i-1}{i}x^i$, $(1-x)^{-1} = \sum_{w=0}^{\infty}x^w$ for $|x|<1$ and, $exp(z) = \sum_{t=0}^{\infty}\frac{z^n}{t!}$, we have: The density of the OBIII-TIIGE-G is

$$f(x;\alpha,\lambda,\beta,k,\phi) \;=\; \sum_{p=0}^{\infty}\eta_{p+1}g_{p+1}, \tag{11}$$

where $g_{p+1} = (p+1)g(x;\phi)G^p(x;\phi)$ defines the exponentiated-G (Expo-G) distribution, $(p+1)$ is the power parameter and

$$\eta_{p+1} = \beta k\lambda\alpha \sum_{i,j,l,m=0}^{\infty} (-1)^p \binom{k+i}{i} \binom{\beta(i+1)+j}{j} \binom{\alpha k+m-1}{m} \times \binom{m-(\alpha+1)}{p} \frac{-\lambda[\beta(i+1)+j]^k}{k!} \frac{1}{p+1}. \quad (12)$$

Consequently, the OBIII-TIIGE-G FoD can be represented as an infinite linear combination of Expo-G densities, from which various statistical properties, including order statistics, probability weighted moments, and entropy can be derived.

3.3 Moments, Moment generating function and incomplete moments

Moments including the mean, variance, skewness, and kurtosis quantify a distribution's central tendency, dispersion, asymmetry, and tail behavior. They are also useful in parameter estimation, hypothesis testing, and comparative analysis across distributions in fields like engineering and physics.

Suppose W_{p+1} represents an Expo-G distributed random variable with a power parameter $(p+1)$, then the r^{th} moment of the OBIII-TIIGE-G FoD can be expressed as

$$E(X^r) = \sum_{m=0}^{\infty} \eta_{p+1} E(W_{p+1}^r),$$

where $E(W_{p+1}^r)$ represents the r^{th} moment of W_{p+1}, and η_{p+1} is defined in Equation (12). The r^{th} incomplete moment can be derived as

$$I_X(t) = \int_0^t x^r f(x)dx = \sum_{p=0}^{\infty} \eta_{p+1} I_{p+1}(t; r, \phi),$$

where $I_{m+1}(t; r, \phi) = \int_0^t x^r g_{m+1}(x; \phi)dx$ defines the incomplete moment of W_{m+1}. Additionally, the moment generating function (mgf) of X is

$$M_X(t) = \sum_{m=0}^{\infty} \eta_{m+1} E(e^{tW_{m+1}}),$$

with $E(e^{tW_{m+1}})$ representing the mgf of W_{m+1}, and η_{j+1} is specified in Equation (12). The derivation of incomplete moments is integral to the formulation of Bonferroni and Lorenz curves, which serve as foundational instruments for examining income disparity, social welfare, and financial risk across diverse disciplines.

4 Some special cases

This section presents some particular cases of OBIII-TIIGE-G FoD by specifying $G(x;\phi)$ and $g(x;\phi)$ in Equations (5) and (16). The half logistic and Lindley distributions serve as parent distributions in this paper.

4.0.1 Odd Burr III-type II general exponential-half logistic distribution

Let the half logistic distribution with the cdf and pdf given by $G(x) = \frac{1-\exp(-x)}{1+\exp(-x)}$ and $g(x) = \frac{2\exp(-x)}{(1+\exp(-x))^2}$ as baseline distribution, for $x > 0$, we have the odd Burr III-type II general exponential-half logistic (OBIII-TIIGE-HL) distribution with cdf

$$F(x;\alpha,\lambda,\beta,k) = \left[1+\left(\frac{\exp\left(\lambda\left[1-\left(\frac{2\exp(-x)}{1+\exp(-x)}\right)^{-\alpha}\right]\right)}{1-\exp\left(\lambda\left[1-\left(\frac{2\exp(-x)}{1+\exp(-x)}\right)^{-\alpha}\right]\right)}\right)^{\beta}\right]^{-k}, \quad (13)$$

and pdf

$$\begin{aligned} f(x;\alpha,\lambda,\beta,k) &= \frac{\beta k\lambda\alpha(2\exp(-x))^{-\alpha}}{(1+\exp(-x))^{1-\alpha}} \frac{\left[\exp\left(\lambda\left[1-\left(\frac{2\exp(-x)}{1+\exp(-x)}\right)^{-\alpha}\right]\right)\right]^{\beta}}{\left[1-\exp\left(\lambda\left[1-\left(\frac{2\exp(-x)}{1+\exp(-x)}\right)^{-\alpha}\right]\right)\right]^{\beta-1}} \\ &\times \left[1+\left(\frac{\exp\left(\lambda\left[1-\left(\frac{2\exp(-x)}{1+\exp(-x)}\right)^{-\alpha}\right]\right)}{1-\exp\left(\lambda\left[1-\left(\frac{2\exp(-x)}{1+\exp(-x)}\right)^{-\alpha}\right]\right)}\right)^{\beta}\right]^{-k-1}. \quad (14) \end{aligned}$$

for $\alpha,\lambda,\beta,k > 0$ and $x > 0$.

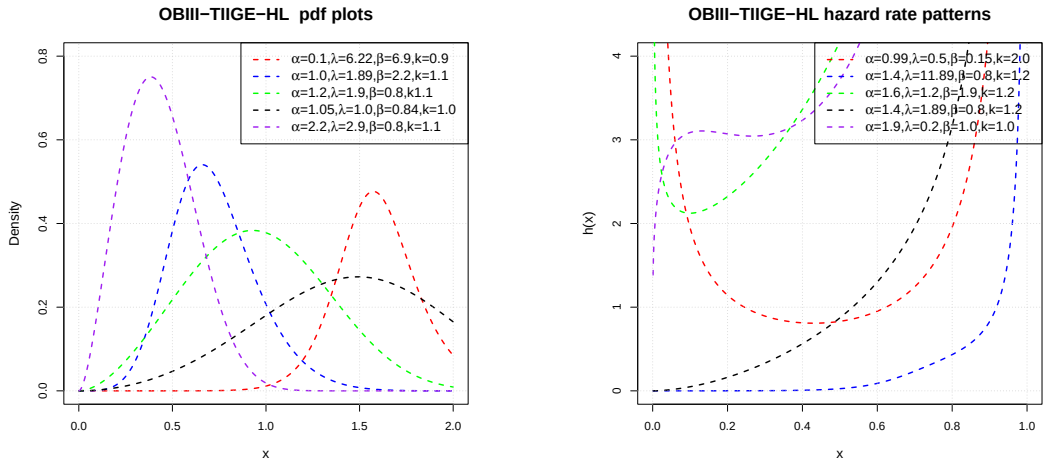

(a) (b)

Figure 1: Some plots of the OBIII-TIIGE-HL distribution's density and hrf

The density plots presented in Figure 1 suggest that the pdf of the OBIII-TIIGE-HL is capable of capturing various data behaviours including positively-skewed, negatively-skewed, and near symmetric geometries. The hrf plots illustrate a variety of hazard rate patterns, encompassing both monotonic and non-monotonic trends.

4.0.2 Odd Burr III-type II general exponential-Lindley (OBIII-TIIGE-Lin) distribution

Considering the Lindley distribution with the cdf and pdf given by $G(x;c) = 1-\left(1+\frac{cx}{1+c}\right)\exp(-cx)$ and $g(x;c) = \frac{c^2}{1+c}(1+x)\exp(-cx)$ as baseline distribution, for $x, c > 0$, we have the OBIII-TIIGE-Lin distribution with cdf

$$F(x;\alpha,\lambda,\beta,k,c) = \left[1+\left(\frac{\exp\left(\lambda\left[1-\left(\left(1+\frac{cx}{1+c}\right)\exp(-cx)\right)^{-\alpha}\right]\right)}{1-\exp\left(\lambda\left[1-\left(\left(1+\frac{cx}{1+c}\right)\exp(-cx)\right)^{-\alpha}\right]\right)}\right)^{\beta}\right]^{-k}, \tag{15}$$

and pdf

$$
\begin{aligned}
f(x;\alpha,\lambda,\beta,k,c) &= \frac{\beta k\lambda\alpha c^2}{1+c}(1+x)\exp(-cx)\left(\left(1+\frac{cx}{1+c}\right)\exp(-cx)\right)^{-(\alpha+1)} \\
&\times \frac{\left[\exp\left(\lambda\left[1-\left(\left(1+\frac{cx}{1+c}\right)\exp(-cx)\right)^{-\alpha}\right]\right)\right]^{\beta}}{\left[1-\exp\left(\lambda\left[1-\left(\left(1+\frac{cx}{1+c}\right)\exp(-cx)\right)^{-\alpha}\right]\right)\right]^{\beta-1}} \\
&\times \left[1+\left(\frac{\exp\left(\lambda\left[1-\left(\left(1+\frac{cx}{1+c}\right)\exp(-cx)\right)^{-\alpha}\right]\right)}{1-\exp\left(\lambda\left[1-\left(\left(1+\frac{cx}{1+c}\right)\exp(-cx)\right)^{-\alpha}\right]\right)}\right)^{\beta}\right]^{-k-1} \quad (16)
\end{aligned}
$$

respectively, for $\alpha, \lambda, \beta, k, c, x > 0$.

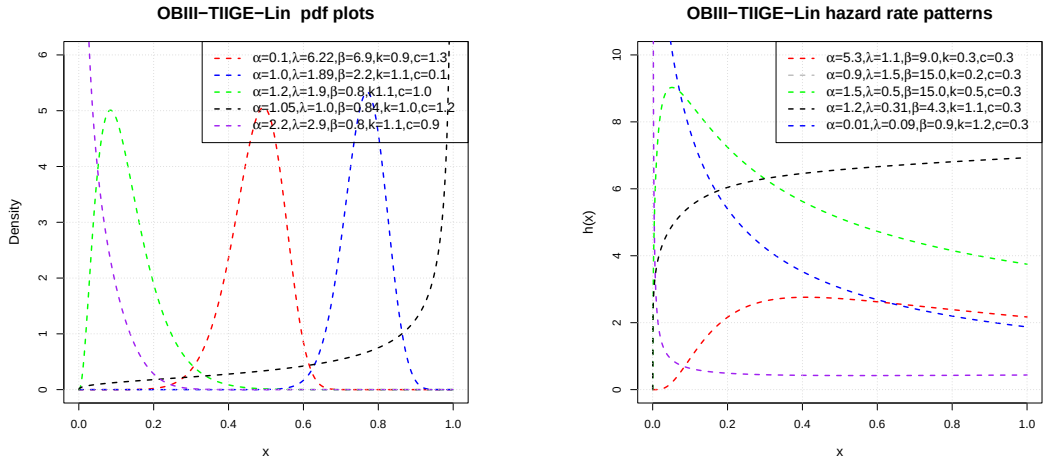

(a) (b)

Figure 2: Some plots of the OBIII-TIIGE-Lin distribution's density and hrf

The density plots presented in Figure 2 suggest that the pdf of the OBIII-TIIGE-HL is capable of capturing various density geometries including J-shaped, right-skewed, near symmetric and left-skewed.

5 Maximum Likelihood Estimation

Given a random sample of size n, where each observation x_i adheres to the OBIII-TIIGE-G family of distributions, and considering $\Delta = (\alpha, \lambda, \beta, k, \phi)^T$ as the parameter vector, the log-likelihood function, $\ell(\Delta)$, is

$$
\begin{aligned}
\ell(\Delta) &= n\ln(\beta k\lambda\alpha) + \sum_{i=1}^{n}\ln g(x_i;\phi) - (\alpha+1)\sum_{i=1}^{n}\ln\left(\bar{G}(x_i;\phi)\right) \\
&+ \sum_{i=1}^{n}\beta\lambda\left[1-\left(\bar{G}(x_i;\phi)\right)^{-\alpha}\right] \\
&- (\beta-1)\sum_{i=1}^{n}\ln\left[1-\exp\left(\lambda\left[1-\left(\bar{G}(x_i;\phi)\right)^{-\alpha}\right]\right)\right] \\
&- (k+1)\sum_{i=1}^{n}\ln\left[1+\left(\frac{\exp\left(\lambda\left[1-\left(\bar{G}(x_i;\phi)\right)^{-\alpha}\right]\right)}{1-\exp\left(\lambda\left[1-\left(\bar{G}(x_i;\phi)\right)^{-\alpha}\right]\right)}\right)^{\beta}\right]. \quad (17)
\end{aligned}
$$

The numerical solution of the nonlinear equations $\left[\frac{\partial\ell}{\partial\alpha}, \frac{\partial\ell}{\partial\lambda}, \frac{\partial\ell}{\partial\beta}, \frac{\partial\ell}{\partial k}, \frac{\partial\ell}{\partial\phi_q}\right]^T = \mathbf{0}$ using iterative methods in R for a specific baseline cdf $G(x;\nu)$, yields the ML estimates of a, b, β and ν_k. Visit the **web appendix** for individual components of the score vector.

It is important to highlight that in order to obtain confidence intervals for the parameters $(\alpha, \lambda, \beta, k, \phi_q)$ and perform hypothesis tests based on Equation (17), it is necessary to have access to the observed information matrix, which can be calculated as follows:

$$
J(\mathbf{\Delta}) = \begin{bmatrix}
J_{\alpha\alpha}(\mathbf{\Delta}) & J_{\alpha\lambda}(\mathbf{\Delta}) & J_{\alpha\beta}(\mathbf{\Delta}) & J_{\alpha k}(\mathbf{\Delta}) & J_{\alpha\phi}(\mathbf{\Delta}) \\
J_{\lambda\alpha}(\mathbf{\Delta}) & J_{\lambda\lambda}(\mathbf{\Delta}) & J_{\lambda\beta}(\mathbf{\Delta}) & J_{\lambda k}(\mathbf{\Delta}) & J_{\lambda\phi}(\mathbf{\Delta}) \\
J_{\beta\alpha}(\mathbf{\Delta}) & J_{\beta\lambda}(\mathbf{\Delta}) & J_{\beta\beta}(\mathbf{\Delta}) & J_{\beta k}(\mathbf{\Delta}) & J_{\beta\phi}(\mathbf{\Delta}) \\
J_{k\alpha}(\mathbf{\Delta}) & J_{k\lambda}(\mathbf{\Delta}) & J_{k\beta}(\mathbf{\Delta}) & J_{kk}(\mathbf{\Delta}) & J_{k\phi}(\mathbf{\Delta}) \\
J_{\phi\alpha}(\mathbf{\Delta}) & J_{\phi\lambda}(\mathbf{\Delta}) & J_{\phi\beta}(\mathbf{\Delta}) & J_{\phi k}(\mathbf{\Delta}) & J_{\phi\phi}(\mathbf{\Delta})
\end{bmatrix}, \quad (18)
$$

where $J_{i,j}(\mathbf{\Delta}) = -\frac{\partial^2\ell_n(\mathbf{\Delta})}{\partial i\partial j}$, $i, j = \alpha, \lambda, \beta, k$, and ϕ is a q component vector of baseline parameters. Under the usual regularity assumptions (see Ferguson [6]), as the sample size n approaches infinity, the estimated parameter vector $\hat{\mathbf{\Delta}}$ follows an asymptotic normal distribution, that is, $\hat{\mathbf{\Delta}} \sim N_{4+p}(\underline{0}, I^{-1}(\mathbf{\Delta}))$. Here, $I(\mathbf{\Delta})$ denotes the anticipated information matrix. Importantly, this asymptotic behavior persists even when the expected information matrix $I(\mathbf{\Delta})$ is substituted with the observed information matrix $J(\hat{\mathbf{\Delta}})$ computed at the estimated parameter vector $\hat{\mathbf{\Delta}}$.

5.1 Simulations

In order to evaluate the effectiveness of MLEs, a simulation study was performed. The results obtained from this simulation are displayed in Table 1,

providing an overview of the findings. We simulated for n= 25, 50, 100, 200, 400, 800 and 1000 and for N=3000 from the OBIII-TIIGE-HL distribution. The absolute bias (AbBIAS) and root mean square error (RtMSE) for an estimated parameter, say $(\hat{k})$, are

$$AbBIAS(\hat{k}) = \left| \frac{\sum_{i=1}^{N} \hat{k}_i}{N} - k \right|, \quad \text{and} \quad RtMSE(\hat{k}) = \sqrt{\frac{\sum_{i=1}^{N} (\hat{k}_i - k)^2}{N}},$$

respectively.

The simulation study evaluates the performance of MLEs for the OBIII-TIIGE-HL distribution, demonstrating their consistency and efficiency. As the sample size increases, the mean estimates of the parameters (α, λ, β, and k) converge toward their true values, while the RMSEr and AbBIAS decrease significantly. This trend holds across various parameter combinations, indicating that the MLEs are asymptotically unbiased and provide reliable estimates. The results also reveal that the OBIII-TIIGE-HL distribution produces efficient parameter estimates, even for smaller sample sizes, though the accuracy improves substantially with larger datasets. The reduction in estimation errors highlights the precision and stability of the estimators, making the OBIII-TIIGE-HL distribution a robust choice for modeling data.

Table 1: Monte Carlo Simulation Results for OBIII-TIIGE-HL: Mean, RtMSE, and AbBias

		$\alpha = 1.4, \lambda = 0.01, \beta = 2.4, k = 2.0$			$\alpha = 1.4, \lambda = 0.01, \beta = 0.3, k = 1.4$		
	n	Mean	RtMSE	AbBIAS	Mean	RtMSE	AbBIAS
α	25	2.1778	3.5842	0.7778	1.6462	1.7055	0.2462
	50	2.0458	2.2535	0.6458	1.6138	0.7370	0.2138
	100	1.5586	0.6845	0.1586	1.6062	0.6527	0.2062
	200	1.4616	0.2191	0.0616	1.5716	0.4637	0.1716
	400	1.4443	0.1226	0.0443	1.5058	0.2439	0.1058
	800	1.4308	0.0949	0.0308	1.4623	0.1222	0.0623
	1000	1.4265	0.0898	0.0265	1.4550	0.1094	0.0550
λ	25	0.0221	0.0482	0.0121	0.0136	0.0154	0.0036
	50	0.0214	0.0405	0.0114	0.0131	0.0086	0.0031
	100	0.0129	0.0171	0.0029	0.0126	0.0055	0.0026
	200	0.0104	0.0056	0.0010	0.0124	0.0045	0.0024
	400	0.0110	0.0025	0.0004	0.0114	0.0029	0.0014
	800	0.0102	0.0023	0.0003	0.0108	0.0013	0.0008
	1000	0.0103	0.0021	0.0002	0.0107	0.0012	0.0007
β	25	2.7904	0.3758	0.3904	0.322	0.1264	0.0220
	50	2.6809	0.3116	0.2809	0.3110	0.1215	0.0110
	100	2.5780	0.1629	0.1780	0.3098	0.0786	0.0098
	200	2.4654	0.0591	0.0654	0.3062	0.0495	0.0062
	400	2.4310	0.0564	0.0310	0.3022	0.0121	0.0021
	800	2.4195	0.0345	0.0195	0.3013	0.0073	0.0013
	1000	2.4003	0.0285	0.0003	0.3004	0.0061	0.0004
k	25	2.3891	0.3628	0.3891	1.3539	0.1361	0.0405
	50	2.3829	0.3363	0.3830	1.3695	0.1338	0.0305
	100	2.3730	0.1864	0.3730	1.3783	0.1140	0.0217
	200	2.3687	0.1203	0.3687	1.3879	0.0856	0.0121
	400	2.3355	0.0792	0.3355	1.3908	0.0491	0.0092
	800	2.2422	0.0671	0.2422	1.3977	0.0291	0.0023
	1000	2.1854	0.0574	0.1855	1.4001	0.0272	0.0001

6 Applications

The objective of this section is to demonstrate the practicality and adaptability of the OBIII-TIIGE-G FoD, with a particular emphasis on its member, the OBIII-TIIGE-HL distribution. This special case is highlighted for its superiority over several non-nested models. To evaluate model performance, various goodness-of-fit (GoF) statistics were employed, including : -2 log-likelihood ($-2\log(L)$), Akaike Information Criterion (AIC), Consistent Akaike Information Criterion (CAIC), Bayesian Information Criterion (BIC), and the Kolmogorov-Smirnov (K-S) statistics along with its p-value. The model that demonstrates lower statistics and the highest K-S p-value is considered the best at capturing the characteristics of the data.

Parameter estimates accompanied by their respective standard errors (SEs), indicated within parentheses were presented for all analyzed datasets. To verify the identifiability of parameter estimates, profile likelihood plots were constructed. The model validation was further supported through multi-faceted graphical diagnostics, including: (i) violin plots, (ii) fitted probability density plots, (iii) probability-probability (P-P) plots, (iv) empirical cumulative distribution function curves (ECDFs), (v) Kaplan-Meier (K-M) survival curves, and (vi) scaled total time on test (TTT) scaled plots.

In our analysis, we conducted a comparative analysis of the OBIII-TIIGE-HL distribution against six alternative non-nested models, which included Burr and half-logistic extensions. The pdf of the contending models are given below.

(a) The pdf of the odd exponentiated half logistic Burr XII (HL-BXII) by Aldahlan and Afify [2] is given by:

$$\begin{aligned} f(x;\alpha,\beta,\delta,c) &= 2\alpha\beta\delta c x^{\delta-1}\exp\left\{\beta\left[1-\left(1+x^{\delta}\right)^{c}\right]\right\} \\ &\times \left(1-\exp\left\{\beta\left[1-\left(1+x^{\delta}\right)^{c}\right]\right\}\right)^{\alpha-1} \\ &\times \left[\left(1+x^{\delta}\right)^{-c+1}\left(1+\exp\left\{\beta\left[1-\left(1+x^{\delta}\right)^{c}\right]\right\}\right)^{\alpha+1}\right]^{-1}, \end{aligned}$$

where α, β, δ, c are positive parameters.

(b) The pdf of the exponentiated half logistic odd Burr III log-logistic (EHL-OBIII-LLOG) distribution by Oluyede et al. [15] is

$$\begin{aligned} f(x;a,b,\alpha,c) &= 2\alpha a b\left[(1+Q^{-a})^{-b}\right]^{\alpha-1}(1+Q^{-a})^{-b-1} \\ &\times \left(1-\left[1-(1+Q^{-a})^{-b}\right]\right)^{-(\alpha+1)}Q^{-a-1} \\ &\times \frac{cx^{c-1}(1+x^{c})^{-2}}{((1+x^{c})^{-1})^{2}}, \end{aligned}$$

where $Q = \left[\frac{[1-(1+x^{\lambda})^{-2}]^{\alpha}}{1-[1-(1+x^{\lambda})^{-2}]^{\alpha}}\right]^{\alpha}$ for $a, b, \alpha, c > 0$ and $x > 0$.

(c) The pdf of the Topp-Leone odd Burr log-logistic Weibull (TL-OBIII-LLoG) distribution developed by Moakofi et al. [10] is

$$\begin{aligned} f(x;\alpha,\beta,b,\lambda) &= 2\alpha\beta b\left\{1-\left(1-\left[1+\left(\frac{1-(1+x^{\lambda})^{-1}}{1+x^{\lambda})^{-1}}\right)^{-\alpha}\right]^{-\beta}\right)^{2}\right\}^{b-1} \\ &\times \left(1-\left[1+\left(\frac{1-(1+x^{\lambda})^{-1}}{1+x^{\lambda})^{-1}}\right)^{-\alpha}\right]^{-\beta}\right)\frac{\lambda x^{\lambda-1}(1+x^{\lambda})^{-2}}{(1+x^{\lambda})^{-1}} \\ &\times \left[1+\left(\frac{1-(1+x^{\lambda})^{-1}}{1+x^{\lambda})^{-1}}\right)^{-\alpha}\right]^{-\beta-1}\left(\frac{1-(1+x^{\lambda})^{-1}}{1+x^{\lambda})^{-1}}\right)^{-\alpha-1}, \end{aligned}$$

for $\alpha, \beta, b, \lambda > 0$ and $x > 0$.

(d) The exponentiated half logistic-generalized log-logistic Poisson (EHL-LLOGP) pdf is given by Chipepa et al. [5]

$$\begin{aligned} f(x;\lambda,\beta,\delta,\theta) &= \frac{2\lambda\delta\beta\theta^{\lambda-1}(1+x^{\lambda})^{(}-\beta+1)[1-(1+x^{\lambda})^{(}-\beta)]^{\delta-1}}{[1+(1+x^{\lambda})^{(}-\beta)]^{\delta+1}} \\ &\times \frac{\exp\left(\theta\left[1-\left(\frac{1-(1+x^{\lambda})^{(}-\beta)}{1+(1+x^{\lambda})^{(}-\beta}\right)^{\delta}\right]\right)}{\exp(\theta)-1}, \end{aligned}$$

for $\lambda, \beta, \delta, \theta > 0$ and $x > 0$.

(e) The pdf of the type II exponentiated half-logistic-Topp-Leone-Weibull Poisson (TIIEHL-TL-WP) developed by Moakofi et al. [12] is

$$\begin{aligned} f(x;a,b,\theta,\lambda) &= 4ab\theta\lambda x^{\lambda-1}(\exp(-x^{\lambda}))^{2}\frac{[1-\exp(-2x^{\lambda})]^{b-1}}{(1+[1-\exp(-2x^{\lambda})]^{b})^{a+1}} \\ &\times (1+[1-\exp(-2x^{\lambda})]^{b})^{a-1}\frac{\theta^{\frac{[1-\exp(-2x^{\lambda})]^{b}}{[1+\exp(-2x^{\lambda})]^{b}}}}{\exp(\theta-1)}, \end{aligned}$$

for $a, b, \theta, \lambda > 0$ and $x > 0$.

(f) The pdf of the odd Burr III Lomax distribution (OBIII-L) developed by Jamal et al. [8] is

$$\begin{aligned} f(x;\beta,\alpha,c,k) &= ck\frac{x}{\beta}\left(1+\frac{x}{\beta}\right)^{-\alpha-1}\frac{[(1+\frac{x}{\beta})^{-\alpha}]^{c-1}}{[1-(1+\frac{x}{\beta})^{-\alpha}]^{c+1}} \\ &\times \left[1+\left(\frac{[(1+\frac{x}{\beta})^{-\alpha}]}{[1-(1+\frac{x}{\beta})^{-\alpha}]}\right)^{c}\right]^{-k-1}, \end{aligned}$$

for $x; \beta, \alpha, c, k > 0$ and $x > 0$.

6.1 Carbon fiber data

The following censored (in Gba) values about the breaking stress of carbon fibers discussed by Nichols and Padgett [13] and also analyzed by Arshad et al. [4]. The dataset is included in the web appendix.

Table 2: Parameter estimates and GoF statistics for carbon fiber data

									Statistics	
Distribution	Estimates and SEs				-2log(L)	AIC	CAIC	BIC	K−S	p−value
	α	λ	β	k						
OBIII-TIIGE-HL	0.3296	133.6200	0.0172	7.6405	171.0683	179.0683	179.7240	187.8269	0.0655	0.9397
	(0.1272)	(2.06×10^{-4})	(0.0108)	(1.7177)						
	α	β	δ	c						
HL-BXII	0.4778	0.0105	0.4599	0.5870	202.6678	210.6678	211.3235	219.4264	0.1237	0.2646
	(0.0784)	(0.0061)	(0.9086)	(0.0827)						
	a	b	α	c						
EHL-OBIII-LLOG	7.6735	1.7075	2.4423	0.3326	212.1413	220.1413	220.7970	228.8999	0.1865	0.0203
	(1.09×10^{-3})	(1.1301)	(1.4136)	(0.0252)						
	α	β	b	λ						
TL-OBIII-LLOG	99.2650	0.2015	225.4800	0.0122	223.2240	231.2240	237.8799	239.9828	0.1941	0.0138
	(1.10×10^{-7})	(0.0149)	(7.22×10^{-6})	(8.96×10^{-4})						
	δ	β	λ	θ						
EHL-LLOGP	9.9783	2.2441	1.3484	2.42×10^{-8}	211.6947	219.6947	220.3505	228.4533	0.1919	0.0155
	(2.4250)	(1.9488)	(1.4791)	(1.72×10^{-6})						
	β	α	c	k						
OBIII-L	2.80×10^{3}	1.72×10^{3}	0.9645	8.5235	190.6470	198.6471	199.3028	207.4057	0.1483	0.1097
	(3.50×10^{-3})	(1.22×10^{-6})	(0.0746)	(1.3954)						
	a	b	θ	λ						
TIIEHL-TL-WP	3.21×10^{-3}	1.9743	131.1000	0.2041	225.8241	233.8241	234.2398	245.3424	0.3341	0.0035
	(5.30×10^{-4})	(0.4819)	(1.41×10^{-4})	(0.0255)						

The MLEs along with their corresponding standard errors (SEs) (in parentheses) are displayed in Table 2. The GoF results from the table show that the OBIII-TIIGE-HL model fits the data better compared to its competitors. The 95% asymptotic confidence intervals (ACI) for the parameters of the OBIII-TIIGE-HL distribution are $\alpha \in (0.3296 \pm 0.2493)$, $\lambda \in (133.6200 \pm 4.04 \times 10^{-4})$, $\beta \in (0.0172 \pm 0.0213$, and $k \in (7.6405 \pm 3.3667)$, respectively. The parameters of the OBIII-TIIGE-HL model on carbon fiber data are uniquely identifiable, as depicted in Figure 3.

The violin plot in Figure [4] (a) shows that the data is almost symmetric and the P-P plot in in Figure [4] (b) shows that the model provides a good fit to the data. The TTT-scaled plot in Figure [4] (c) suggest that the data has an increasing hazard rate.

The histogram shown in Figure [5] (a) illustrate how the fitted OBIII-TIIGE-HL distribution outcompete the contending models in terms of fit. The ECDF and K-M survival curve shown in Figure [5] (b) and (c) shows how the OBIII-TIIGE-HL outperforms the contending models in aligning the observed and fitted curves.

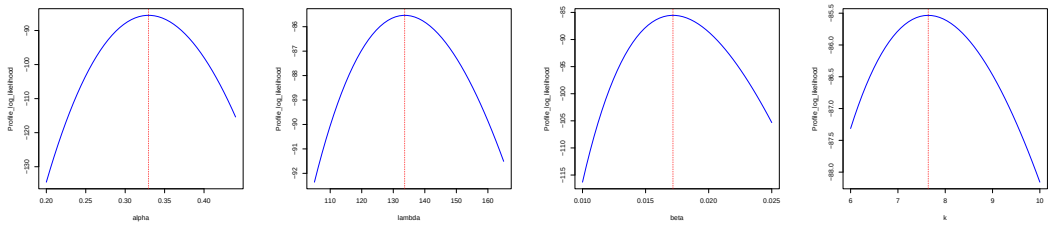

(a) (b) (c) (d)

Figure 3: Profile log-likelihood plots for carbon fiber data

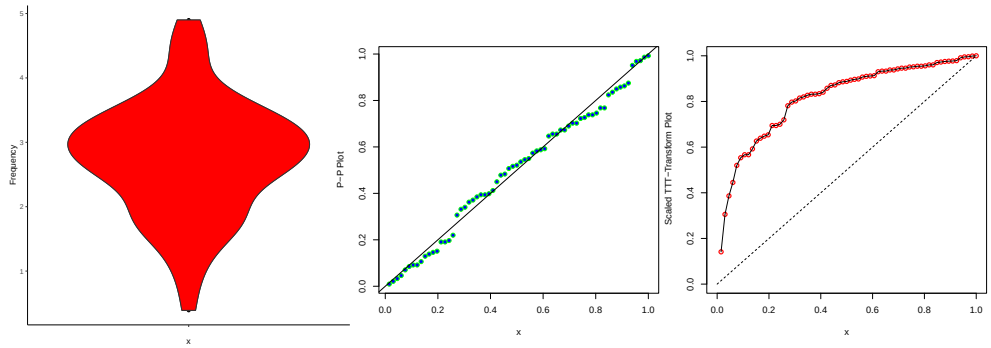

(a) Violin plot (b) P-P plot (c) ECDF curve

Figure 4: Graphs illustrating the (a) violin plot, (b) P-P plot and (c) TTT-scaled plot for carbon fiber data

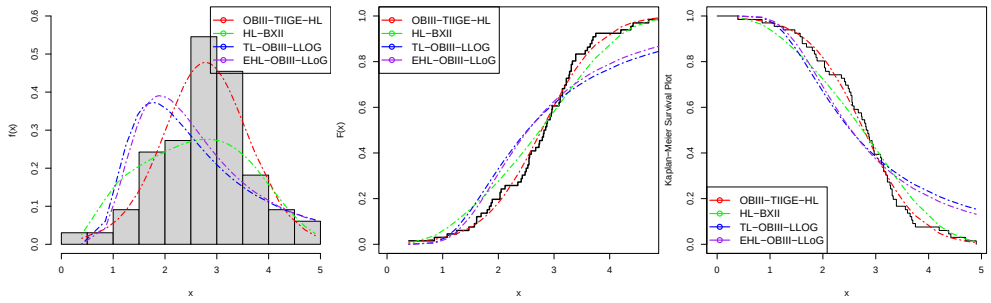

(a) K-M survival curve (b) ECDF curve (c) K-M survival curve

Figure 5: Fitted density plot, ECDF curve and K-M survival curve for carbon fiber data

6.2 Silicon nitride data

The following symmetric set of a data consists of fracture toughness from the silicon nitride. The data can be downloaded directly from the web-site `http://www.ceramics.nist.gov/srd/summary/ftmain.htm` and also studied by Nichols and Padgett [13] and Moakofi and Oluyede [11] . The data is provided in the web appendix.

Table 3: Parameter estimates and GoF statistics for silicon nitride data

					Statistics					
Distribution	Estimates and SEs				-2log(L)	AIC	CAIC	BIC	K−S	p−value
	α	λ	β	k						
OBIII-TIIGE-HL	0.4215	16.2046	0.0396	8.1643	338.7132	346.7132	347.0641	357.8297	0.0564	0.843
	(0.0793)	(1.50×10^{-3})	(1.0180)	(1.5983)						
	α	β	δ	c						
HL-BXII	0.4526	2.93×10^{-5}	150.713	0.0427	385.3768	393.3768	393.7277	404.4933	0.0909	0.2787
	(4.89×10^{-5})	(1.72×10^{-5})	(5.79×10^{-7})	(2.28×10^{-3})						
	a	b	α	c						
EHL-OBIII-LLOG	4.0673	30.9214	1.8146	0.8693	408.0323	416.0323	416.3831	427.1488	0.1895	0.0042
	(0.0110)	(17.9309)	(0.7607)	(0.0496)						
	α	β	b	λ						
TL-OBIII-LLOG	20.0830	69.6990	0.5826	0.1285	395.8317	403.8317	404.1826	414.9482	0.1848	0.0059
	(3.17×10^{-3})	(6.67×10^{-4})	(0.0961)	(4.96×10^{-3})						
	δ	β	λ	θ						
EHL-LLOGP	234.3900	3.9749	1.0084	8.76×10^{-9}	408.9203	416.9203	417.2712	428.0368	0.1900	0.0037
	(1.50×10^{-3})	(0.2507)	(0.0947)	(6.87×10^{-3})						
	β	α	c	k						
OBIII-L	8.15×10^{4}	2.65×10^{4}	2.1201	6.8385	382.4742	390.4742	390.8252	401.5908	0.1619	0.0932
	(1.35×10^{-4})	(4.17×10^{-4})	(0.1234)	(0.7766)						
	a	b	θ	λ						
TIIEHL-TL-WP	3.78×10^{-3}	2.0860	103.6100	0.1775	408.3469	416.3469	416.6978	427.4634	0.1794	0.0534
	(4.64×10^{-4})	(0.3883)	(2.43×10^{-4})	(0.0167)						

The MLEs along with their corresponding standard errors (SEs) (in parentheses) are displayed in Table 3. The GoF results from the table show that the OBIII-TIIGE-HL model provides a better fit to the silicone nitride data. The 95% ACI for the parameters of the OBIII-TIIGE-HL distribution are $\alpha \in (0.4215 \pm 0.1504)$, $\lambda \in (16.2046 \pm 2.95 \times 10^{-3})$, $\beta \in (0.0396 \pm 0.0354)$, and $k \in (8.1643 \pm 3.1326)$, respectively. The parameters of the OBIII-TIIGE-HL model on silicone nitride data are uniquely identifiable, as depicted in Figure 6.

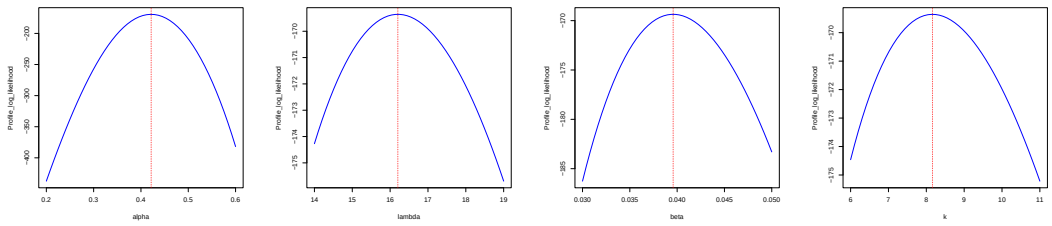

(a) (b) (c) (d)

Figure 6: Profile log-likelihood plots for silicon nitride data

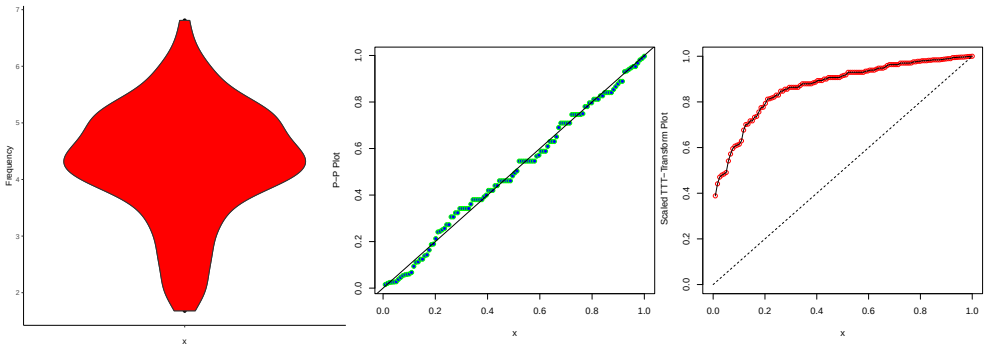

(a) Violin plot (b) P-P plot (c) ECDF curve

Figure 7: Graphs illustrating the (a) violin plot, (b) fitted densities and (c) ECDF plots for silicon nitride data

The violin plot in Figure [7] (a) depicts that the silicon nitride data is almost symmetric and the P-P plot in in Figure [7] (b) shows that the OBIII-TIIG-HL distribution provides a good fit to the data. Figure [7] (c) shows that the silicone nitride data is monotonically increasing since the plot is concave. The fitted densities plots, ECDF curve and K-M survival curves in

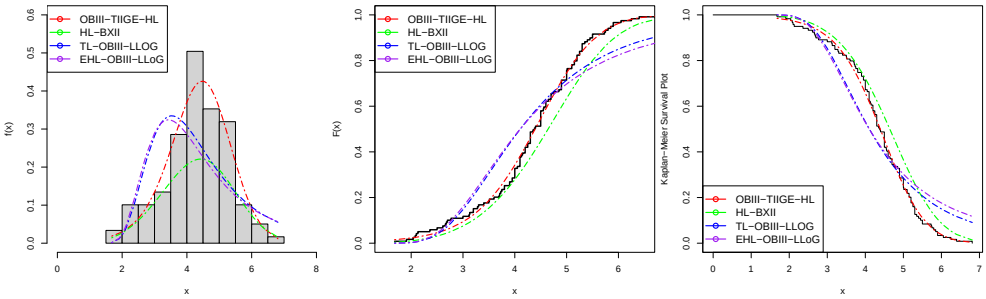

(a) K-M survival curve (b) ECDF curve (c) K-M survival curve

Figure 8: Fitted density plot, ECDF curve and K-M survival curve for silicon nitride data

Figures [8] (a) , (b) and (c) demonstrate that the OBIII-TIGE-HL shows a close correspondence with all the graphs. This corroborates the good-fit of the OBIII-TIGE-HL distribution to silicone nitride data.

7 Concluding remarks and recommendations

The OBIII-TIIGE-G family of distributions represents a significant advancement in statistical modeling, offering unparalleled flexibility to capture diverse

data geometries (symmetric, skewed, J-shaped, and heavy-tailed). By unifying the odd Burr III-G and type II general exponential-G frameworks, this study addresses critical limitations in existing models, particularly their restricted capacity to simultaneously model multi-phase hazard dynamics and closed-form statistical properties. The proposed family's analytical tractability—evidenced by explicit expressions for quantile functions, moments, and hazard rates—enables direct application in reliability engineering, survival analysis, and materials science. Empirical validation through simulations and real-world failure datasets underscores its robustness, with superior goodness-of-fit and parameter identifiability compared to six competing models.

To maximize the impact of this work, the following recommendations are proposed:

- Bayesian estimation: Exploring Bayesian inference methods, such as Markov Chain Monte Carlo (MCMC) techniques, could complement maximum likelihood estimation, particularly for small-sample scenarios.
- Applications beyond engineering: Testing the model's efficacy in finance (e.g., risk assessment), environmental science (e.g., extreme weather events), and healthcare (e.g., disease progression) could uncover new avenues for interdisciplinary utility.
- Tail behavior analysis: Investigating the family's performance in modeling ultra-heavy-tailed or multimodal datasets would further validate its versatility.

This study not only advances distribution theory but also equips researchers and practitioners with a powerful tool to address complex real-world challenges. By bridging gaps in hazard rate modeling and parameter estimation, the OBIII-TIIGE-G family sets a foundation for future innovations in statistical reliability and beyond.

To access the appendix, kindly click on the link provided below:
`https://drive.google.com/file/d/1AYLM9jyRvY9V14fxAbBGA6xIXZ8m7wTH/view?usp=sharing`

References

[1] Afify, A. Z., Cordeiro, G. M., Ibrahim, N. A., Jamal, F., Elgarhy, M., and Nasir, M. A. (2020). The Marshall-Olkin odd Burr III-G family: Theory, estimation, and engineering applications. *IEEE Access*, 9, 4376-4387.

[2] Aldahlan, M., and Afify, A. Z. (2018). The odd exponentiated half-logistic Burr XII distribution. *Pakistan Journal of Statistics and Operation Research*, 14(2), pp. 305-317.

[3] Alizadeh, M., Cordeiro, G. M., Nascimento, A. D. C., Lima, M. C. S., and Ortega, E. M. M. (2017). Odd-Burr generalized family of distributions with some applications. *Journal of Statistical Computation and Simulation*, 87, 367-389.

[4] Arshad, M. Z, Iqbal, M. Z., and Mutairi, A. A. (2021). A comprehensive review of datasets for statistical research in probability and quality control. *Journal of Mathematics and Computer Science*, 11(3), 3663-3728.

[5] Chipepa, F., Chamunorwa, S., Oluyede, B., and Makubate, B.(2022). The exponentiated half logistic-generalized-G power series class of distributions: Properties and applications. *Journal of Probability and Statistical Science*, 20(1), 21–40.

[6] Ferguson, T. S., (1996). A Course in Large Sample Theory. *Chapman & Hall, London.*

[7] Hamedani, G. G., Rasekhi, M., Najibi, S., Yousof, H. M., and Alizadeh, M. (2019). Type II general exponential class of distributions. *Pakistan Journal of Statistics and Operation Research*, 15(2), 503-523.

[8] Jamal, F., Nasir, M. A., Tahir, M. H., and Montazeri, N. H. (2017). The odd Burr-III family of distributions. *Journal of Statistics Applications and Probability*, 6(1), 105-122.

[9] Jamal, F., Bakouch, H. S., and Arslan Nasir, M. (2021). Odd Burr III G-negative binomial family with applications. *Journal of Testing and Evaluation*, 49(5), 3528-3548.

[10] Moakofi, T., Oluyede, B., and Gabanakgosi, M. (2022). The Topp-Leone odd Burr III-G family of distributions: Model, properties and applications. *Statistics Optimization and Information Computing*, pp. 1–27.

[11] Moakofi, T., and Oluyede, B. (2023). The type II exponentiated half-logistic Gompertz-G family of distributions: Properties and applications. *Mathematica Slovaca*, 73(3), 785-810.

[12] Moakofi, T., Oluyede, B., and Chipepa, F. (2021). Type II exponentiated half-logistic-Topp-Leone-G power series class of distributions with applications. *Pakistan Journal of Statistics and Operation Research*, 885-909.

[13] Nichols, M. D and Padgett, W. J. (2006). A bootstrap control chart for Weibull percentiles. *Quality Reliability Engineering*, 22, 141–151.

[14] Nkomo, W., Oluyede, B., and Chipepa, F. (2025). Type I heavy-tailed family of generalized Burr III distributions: properties, actuarial measures, regression and applications. *Statistics in Transition new series*, 26(1), 93-115.

[15] Oluyede, B., Peter, O. P, Nkumbuludzi, N., and Huybrechts, B. (2022). The exponentiated half-logistic odd Burr III-G: Model, properties and applications. *Pakistan Journal of Statistics and Operation Research*, 18(1), 33–57.